NeuroImage 122 (2015) 417–426

Contents lists available at ScienceDirect

NeuroImage

journal homepage: www.elsevier.com/locate/ynimg

MEG—measured auditory steady-state oscillations show high test–retest reliability: A sensor and source-space analysis

H.-R.M. Tan *, J. Gross, P.J. Uhlhaas

Centre for Cognitive Neuroimaging (CCNi), Institute of Neuroscience and Psychology (INP), College of Medical, Veterinary and Life Sciences & College of Science and Engineering, University of Glasgow, 58 Hillhead Street, Glasgow G12 8QB, Scotland, United Kingdom

ARTICLE INFO

Article history:
Received 6 March 2015
Accepted 20 July 2015
Available online 26 July 2015

Keywords:
Test–retest reliability
Auditory steady-state responses (ASSRs)
Magnetoencephalography (MEG)
eLORETA beamforming
5 Hz and 40 Hz amplitude-modulated (AM) tones
Inter-trial phase coherence (ITPC)
Time–frequency analysis

ABSTRACT

Stability of oscillatory signatures across magnetoencephalography (MEG) measurements is an important prerequisite for basic and clinical research that has been insufficiently addressed. Here, we evaluated the test–retest reliability of auditory steady-state responses (ASSRs) over two MEG sessions. The study required participants (N = 13) to detect the rare occurrence of pure tones interspersed within a stream of 5 Hz or 40 Hz amplitude-modulated (AM) tones. Intraclass correlations (ICC; Shrout and Fleiss, 1979) were derived to assess stability of spectral power changes and the inter-trial phase coherence (ITPC) of task-elicited neural responses. ASSRs source activity was estimated using eLORETA beamforming from bilateral auditory cortex. ASSRs to 40 Hz AM stimuli evoked stronger power modulation and phase-locking than 5 Hz stimulation. Overall, spectral power and ITPC values at both sensor- and source-level showed robust ICC values. Notably, ITPC measures yielded higher ICCs (~0.86–0.96) between sessions compared to the assessment of spectral power change (~0.61–0.82). Our data indicate that spectral modulations and phase consistency of ASSRs in MEG data are highly reproducible, providing support for MEG-measured oscillatory parameters in basic and clinical research.

Introduction

Neural oscillations are considered relevant for understanding brain functions and associated cognitive and perceptual processes (Lopes da Silva, 2013; Siegel et al., 2012; Wang, 2010). This is because they establish precise temporal relationships between and within distributed neuronal assemblies and thus contribute to the formation of functional networks (Buzsáki and Watson, 2012; Fries, 2005; Gray and Singer, 1989; Helfrich et al., 2014; Womelsdorf et al., 2007). In addition, rhythmic activity at low (delta/theta/alpha) and high (beta/gamma) frequency ranges facilitate different modes through which these networks can be flexibly established, such as through coupling different frequencies and synchronizing phase-relations between oscillators (Akam and Kullmann, 2014; Canolty and Knight, 2010; Roopun et al., 2008; Siegel et al., 2012). Converging data (e.g. Bartos et al., 2007; Brunel and Wang, 2003; Cardin et al., 2009; Sohal et al., 2009; Traub et al., 1996; see Buzsáki and Wang, 2012 for review) support the view that oscillatory activity at different frequencies reflects the balanced coordination of neuronal excitation and inhibition (E/I) and that imbalances may manifest as cognitive dysfunctions and aberrant rhythmic activity reported in neuropsychiatric disorders, such as schizophrenia (ScZ) and autism spectrum disorders (ASDs) (Gonzalez-Burgos and Lewis, 2008; Schnitzler and Gross, 2005; Uhlhaas and Singer, 2012).

Electro- and magnetoencephalography (EEG/MEG) allow the non-invasive assessment and reconstruction of neural oscillations and their underlying networks through measurement of the synchronous activations of large population of neurons. In contrast to EEG which measures neural activity via scalp electrodes, the weak magnetic fields induced by cortical activity remain undistorted by the various conductivities of head tissues and are detected by the highly sensitive superconducting quantum interference devices (SQUIDs) in MEG. Recent application of MEG in understanding normal rhythmic activity has highlighted the role of frequency-specific neural oscillations in cognitive and perceptual processes (Gross et al., 2013; Rouhinen et al., 2013; Roux et al., 2012; Tan et al., 2013). In addition, there is a growing interest in employing MEG to understand neural oscillations in brain disorders with the potential to yield biomarkers for early detection and diagnosis (e.g. Georgopoulos et al., 2010; Rojas et al., 2011; Sun et al., 2013; Tada et al., 2014).

Despite the widespread application of MEG, there is currently little evidence on the reliability of oscillatory signatures across multiple measurements. This question is important since previous research has indicated that the peak-frequency of neural oscillations, for example, is highly genetically heritable (van Pelt et al., 2012), suggesting that certain signatures of rhythmic activity could constitute a trait-like characteristic or spectral fingerprint (Siegel et al., 2012). In addition, the

* Corresponding author.
E-mail address: Heng-RuMay.Tan@glasgow.ac.uk (H.-R.M. Tan).

http://dx.doi.org/10.1016/j.neuroimage.2015.07.055

possibility to obtain reliable estimates of oscillatory activity across measurements is a prerequisite to employ MEG in longitudinal studies in clinical and non-clinical populations.

To date, the only study which has assessed test–retest reliability of neural oscillations in MEG data is the study by Muthukumaraswamy et al. (2010). The authors reported high intraclass correlation (ICC) values (0.8–0.98) for the peak-frequency of visually elicited gamma (40–60 Hz) band responses across multiple assessments for source-reconstructed MEG signals. Source analysis may yield more stable estimates of MEG activity compared to sensor-derived values as the need for exact positioning of participants under the MEG sensors across repeated recordings is reduced. By comparison, lower ICC values (mean ICC = 0.62) have been obtained for sensor-derived graph-theoretical metrics during rest and an N-back task, despite accounting for continuous head position monitoring (cHPI) (Deuker et al., 2009). However, it is not clear if the more complex metrics used for repeatability assessment, the choice of task or indeed the sensor-based analytical approach were the reason for the comparatively lower ICCs. Supporting the possibility that source-derived parameters may be more robust in MEG data, Lu et al. (2007) reported higher ICCs (≥ 0.8) from dipole-modelling derived P50 during a paired-click paradigm relative to previous reports (Boutros et al., 1991; Cardenas et al., 1993; Jerger et al., 1992; Kathmann and Engel, 1990; Lamberti et al., 1993).

As existing research shows, the reliability of neural oscillations can be assessed under varying contexts. These include spontaneous resting-state activity that is thought to reflect intrinsic neural dynamics and task-elicited oscillatory activity that reflects the neural modulation due to sensory and/or cognitive processing. Depending on whether they time-lock to stimulus onset or emerge with trial-to-trial variability, such task-elicited neural modulations are categorized as 'evoked' or 'induced', respectively (Tallon-Baudry and Bertrand, 1999). The distinct phase-relationship of evoked and induced oscillatory activity is further exemplified in their analytical derivation. Evoked power is estimated by initial trial-averaging prior to spectral decomposition. Spectral power of induced neural oscillations is revealed by first deriving single-trial time–frequency decomposition before trial-averaging, followed by the subtraction of both evoked power and any background components from the resulting power average (David et al., 2006). To further examine whether oscillatory signatures in MEG data, in particular estimates of spectral power and phase consistency, are reliable across measurements and whether source reconstruction improves the test–retest reliability, we examined auditory steady-state responses (ASSRs) across two MEG recordings in healthy volunteers.

Unlike intrinsic oscillatory activity, steady-state responses (SSRs) are established through entraining neuronal populations in response to a temporally modulated sensory stimulus and are therefore a means to probe the integrity of neuronal networks to maintain precisely coordinated temporal activity (Brenner et al., 2009; Regan, 1989). ASSR is commonly elicited using trains of clicks, noise bursts, or amplitude-modulated (AM) tones (Brenner et al., 2009; Galambos et al., 1981; Picton et al., 2003; Ross et al., 2000; 2002). In humans, ASSR recorded by M/EEG is strongest to stimuli presented within the 30–50 Hz range (Azzena et al., 1995; Galambos et al., 1981; Picton et al., 2003) which has been interpreted as a resonance response of networks in auditory cortices (Hamm et al., 2011, 2012; McFadden et al., 2014; Pantev et al., 1996; Ross et al., 2000; see Brenner et al., 2009, for review). In addition, ASSRs have been investigated in psychiatric disorders and reduced amplitude as well as phase consistency of evoked ASSR to 40 Hz stimulation have been observed in ScZ (e.g. Brenner et al., 2003; Hamm et al., 2011; Hirano et al., 2015; Krishnan et al., 2009; Kwon et al., 1999; Light et al., 2006; Spencer et al., 2008; Tada et al., 2014; however, see Hamm et al., 2012) and their first-degree relatives (Hong et al., 2004; Rass et al., 2012) as well as in ASDs (Wilson et al., 2007). Reduced 40 Hz ASSRs in these disorders is consistent with findings of altered cellular parameters affecting E/I balance (Hashimoto et al., 2008; Moyer et al., 2012; Sweet et al., 2009, 2007), supporting the potential clinical utility of the ASSR paradigm in translational research.

At present, test–retest reliability of ASSR parameters has only been reported in EEG data by McFadden et al. (2014), who examined the consistency of ASSRs to 40 Hz amplitude-modulated white noise and 40 Hz click trains in a passive listening task, and observed that inter-trial phase coherence (ITPC) measures of ASSRs may be more reliable compared to spectral signal change. In the current study, we evaluated the reliability of ASSRs to both 5 Hz and 40 Hz AM tones in an attentive listening task paradigm at MEG sensor level and from estimated source signals derived via (eLORETA) beamforming. MEG source estimation employing beamforming may improve signal-to-noise (SNR) and confers an advantage over dipole-fitting (e.g. Lu et al., 2007; McFadden et al., 2014; Teale et al., 2008) through the use of head models based on individual anatomical MRI data. In addition, it facilitates the definition of regions of interests (ROIs), such as the auditory areas, which are important for the generation of ASSRs (Hamm et al., 2011, 2012; McFadden et al., 2014; Pantev et al., 1996; Ross et al., 2000).

Methods

Participants

We evaluated the test–retest reliability of ASSRs in fourteen healthy participants (4 females; mean age (±sd) = 25 (±4) years) over two MEG sessions (range 1–11 days; mean (±sd) = 4 (±3) days apart). Participants were recruited from the University of Glasgow School of Psychology participant pool, provided informed consent prior to the experiment, and were compensated (at the standard rate of £6/hr) for their time. All participants were right-handed (Edinburgh Handedness Test; Oldfield, 1971), characterized by normal hearing and had no known neurological disorders. The experimental protocol, in which the ASSR experiment was part of a battery of sensory processing tasks performed during each MEG session, was approved by the University of Glasgow College of Science and Engineering Ethics Committee.

Prior to each MEG session, scheduled at the same time of the day, each participant filled in a brief questionnaire which assessed differences in caffeine intake, smoking habits, alcohol consumption, and hours of sleep as well as general well-being prior to each measurement. Participants' responses did not differ across sessions (caffeine intake: $t_{13} = -1.8$, $p = 0.096$; sleep hours: $t_{13} = -1$, $p = 0.34$; Wilcoxon signed-rank tests for cigarettes smoked and alcohol intake are both non-significant). Additionally, to control for potential influence of hormonal fluctuations (Griskova-Bulanova et al., 2014), female subjects participated within the first 5–10 days during the follicular phase of their menstrual cycle in both MEG sessions.

Stimuli and task

Three different auditory stimuli, comprising a 1000 Hz pure tone as well as its corresponding 5 Hz and 40 Hz amplitude-modulated (AM) tones, were presented (78 dB SPL). Each tone lasted 2 s long (ITI = ~1.5 s, jittered, which included the baseline of 1 s) and was designed with 10 ms ascending and descending ramps. The tones were generated according to the formula:

$$AM = \sin(2\pi f_c t) * (1 + m * \cos(2\pi f_m t))$$

where f_c is the 1000 Hz carrier frequency, f_m is the frequency of amplitude modulation (i.e. 0 Hz, 5 Hz, or 40 Hz), $m = 1$ is the modulation depth, and t is the sampling time points at 48 KHz sampling frequency.

For each of the 2 runs of the ASSR task, participants mentally noted the rare occurrences (10%) of pure tones interspersed within a stream of 5 Hz or 40 Hz AM tones (see Fig. 1). A total of 120 and 110 tones were presented in the 5 Hz and 40 Hz ASSR runs, respectively. While they were listening to the tones, participants were instructed to keep

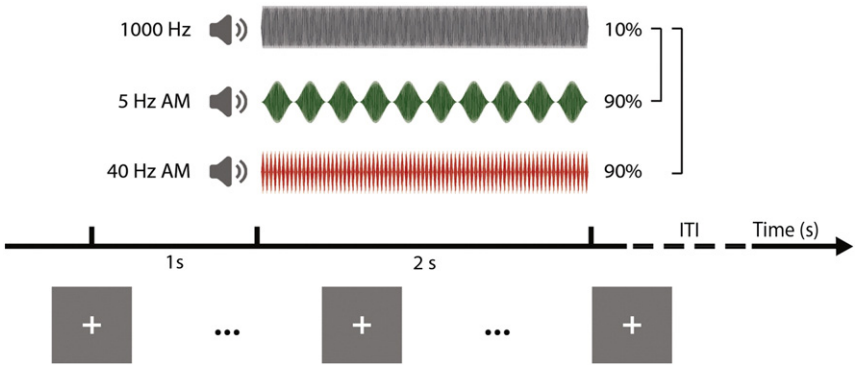

Fig. 1. Experimental paradigm. Three types of auditory stimuli were presented and comprised a 1000 Hz pure tone as well as its 5 Hz and 40 Hz amplitude-modulated (AM) tones. Rare occurrences (10%) of pure tones were interspersed within a stream of 5 Hz or 40 Hz AM tones that make up a block of the ASSR task. Each tone lasted for 2 s long and the ITI between sound presentations is approximately 1.5 s; ITI was slightly jittered to prevent stimuli occurrence prediction.

their eyes fixated on a center cross (projected 186 cm in front) and to report the number of perceived pure tone occurrences at the end of each ASSR run. Trials in which pure tones were presented (i.e. 12 and 11 rare instances for 5 Hz and 40 Hz ASSR runs, respectively) were included to sustain participants' attention but were excluded in the analyses. The sequence of either 5 Hz followed by 40 Hz (or vice versa) experimental runs (~8 min duration; each trial ~3.5 s long) was counterbalanced.

Neuroimaging acquisition

MEG data were acquired using a 248-channel magnetometer system (MAGNES® 3600 WH, 4D-Neuroimaging, San Diego) while participants engaged in the task, sitting upright within an electromagnetically shielded room. For each participant, a suitable MEG seat position was determined and marked during the first session. Every attempt was taken to keep this seat position and the MEG system's helmet (housing the SQUID sensors) in the same configuration prior to each acquisition so as to minimize the variance of participants' head and sensors' positioning across runs and sessions. Head position stability was assessed before and after each acquisition run via five indicator coils attached relative to the (left, right preauricular, and nasion) fiducials and were co-digitized with participants' head shape (FASTRAK®, Polhemus Inc., VT, USA) for subsequent co-registration with individual MRI (1 mm^3 T1-weighted; 3D MPRAGE). The MEG touch-pad response (LUMItouch™, Photon Control Inc., BC, Canada) and eye-tracker (EyeLink 1000; SR Research Ltd., Ontario, Canada) signals were sampled synchronously at 1017.25 Hz, with online 0.1 Hz high-pass filtering.

MEG data processing

All data processing and analyses were performed using Fieldtrip Toolbox functions (http://fieldtrip.fcdonders.nl; Oostenveld et al., 2011) and additional scripts developed within MATLAB® (The MathWorks, Natick, MA). Faulty sensors (mean (± SEM) = 10 ± 2 per session, visually identified) with large signal variance or whose signals were flat were removed and interpolated using nearest-neighbor averaging procedure. One MEG measurement was corrupted by global noise and technical issues during one of the two acquisition sessions. Accordingly, this participant was excluded from the analyses reported here (i.e. N = 13).

Raw MEG signals were epoched from −1000 to +3000 ms relative to stimulus onset (0 ms), with linear trends removed, power-line (50 Hz) notch-filtered, and 'de-noised' relative to reference MEG channel signals. Raw trials were visually inspected and trials with obvious artifacts (muscle, squid jumps, etc.) were excluded. Independent component analysis was used to isolate and to reject ocular movement and cardiac components from the MEG signals. This yielded on average (±SEM) 91.65 (±2.22) artifact-free trials for each ASSR condition per session. As trial numbers could impact on estimates of spectral power change and inter-trial phase coherence (ITPC), the mean (±sd) number of trials for different sessions was examined. Trial numbers for both 5 Hz (sessions 1 = 93.23 (±9.69) trials; session 2 = 96.08 (±7.19) trials) and 40 Hz (session 1 = 90.08 (±5.76) trials; session 2 = 87.23 (±6.81) trials) ASSR conditions did not differ significantly across sessions (repeated-measures t-test for 5 Hz: $t_{13} = -1.16$, $p = 0.27$ and 40 Hz: $t_{13} = 1.51$, $p = 0.16$).

Time–frequency analysis on sensor and source signals

For sensor-level analysis, artifact-free neuromagnetic time series were transformed from axial magnetometer to planar gradient signals (Bastiaansen and Knosche, 2000) prior to time–frequency analyses and subsequently recombined. This procedure allows a more intuitive inference of dipole signals above a source or from axial pick-up coils, which are sensitive to magnetic components oriented normal (cf. tangential) to the head surface, and simplifies its corresponding topographical interpretation. At the source level, we focused on primary auditory areas in the generation of ASSRs based on prior work (Hamm et al., 2011, 2012; McFadden et al., 2014; Pantev et al., 1996; Ross et al., 2000). Virtual sensors' signals were extracted from bilateral superior temporal and Herschl's gyri using individual MNI-normalized source model grid (6 mm resolution) and the eLORETA inverse-solution algorithm (Pascual-Marqui, 2007, 2011); see Fig. $2_{(ii)}$). Multitaper fast-fourier time-frequency decomposition (±2 Hz taper smoothing and 10 ms temporal resolution) was performed on artifact-free epochs for both sensor and source signals (1 Hz resolution from 2 Hz to 50 Hz for the 5 Hz AM stimulus; 2 Hz resolution from 2 Hz to 100 Hz for the 40 Hz AM stimulus).

Spectral power and inter-trial phase coherence

As the ASSR evolves approximately after 240 ms post-stimulus onset (Ross et al., 2002) following the transient response, we considered the period from 500 ms to 2000 ms post-stimulus onset as the stimulus duration of interest (see Fig. 4). Given the known ASSR stimulus frequency, we specifically assessed oscillatory parameters within the narrow frequency range of interest (FOI): 2–8 Hz and 34–46 Hz for the 5 Hz and 40 Hz stimulus conditions (see Supplementary Figs. 1, 2), respectively. All spectral power time series were expressed as relative change to baseline (500 ms prior to auditory stimulus onset; Fig. 4). Instantaneous inter-trial phase coherence (ITPC; Tallon-Baudry et al., 1996) was derived from the complex norm of the time–frequency decomposition with ITPC values ranging from 0 to 1, reflecting zero to near-perfect phase consistency across trials.

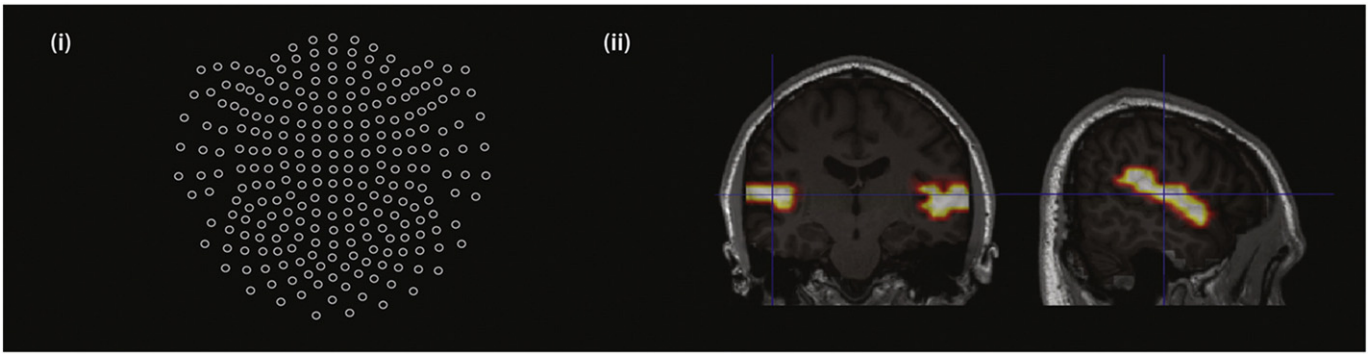

Fig. 2. Description of sensor and source space from which neuromagnetic signals were derived. (i) Two-dimensional sensor array layout of the 4D Neuroimaging (San Diego, USA) MEG system. (ii) Sources delineated within auditory brain regions of interest shown in coronal and sagittal views.

Derivation of oscillatory parameters and reliability analysis

For each ASSR stimulus condition, ITPC and spectral modulation were averaged over the 500–2000 ms window for each frequency. We determined the modulation of the parameters of interest at ASSR stimulus frequency (Fig. 3) by using both a conventional approach of applying a 1st order Gaussian fit on the time-averaged spectral and phase-locking time series (Campbell et al., 2014; Haegens et al., 2014) and without (See Supplementary Results). We calculated the intraclass correlation (ICC; Shrout and Fleiss, 1979) using MatlabCentral file-exhange *ICC.m* function (A. Salarian, 2008, implemented with statistical testing based on McGraw and Wong (1996a, 1996b) to assess the degree of consistency among frequency-specific ASSR measurements (consistency ICC: case 2). Defined as the ratio of between-subject variance and the total variance, ICC assesses the reliability of the repeated measures of an individual's oscillatory parameters by comparing the between-measures variability of each individual to the total variation across all measures and participants. Unlike Pearson's correlation coefficient, which detects the linear association between two (possibly different) measures, ICCs reflect the agreement of a participant's neural measure from one session to another, accounting for the associated variance (McGraw and Wong, 1996). An ICC value of 1 indicates perfect within-subject reliability of neural oscillatory measures derived on differing occasions from the same participants, while an ICC of 0 indicates no reliability. ICCs were assessed for both sensor- and source-derived neuromagnetic signals and for each ASSR stimulus condition. Additionally, we investigated the reliability of absolute power values during baseline and stimulus duration of interest (See Supplementary Results).

Results

The primary focus of the present study was to assess the test–retest reliability of ASSRs at 5 Hz and 40 Hz from MEG sensor and estimated source signals. The overall finding indicated highly significant ICCs (mean ICC = 0.839; ICC range: 0.609–0.964; $p < 0.01$–$p << 0.0001$) on both spectral signal change and ITPC oscillatory measures.

Participants' grand-averaged ASSRs to both 5 Hz and 40 Hz stimuli are shown in Fig. 4 and indicate an enhanced response in the right hemisphere consistent with previous findings (Ross et al., 2005). Stimulus onset elicited a strong but transient evoked low-frequency response in both spectral change (Fig. $4_{(ii),\,(v)}$) and ITPC (Fig. $4_{(iii),\,(vi)}$) values at sensor level and in source space which was followed by a narrow-banded sustained response corresponding to the frequency and duration of the stimulation.

The 40 Hz AM tone elicited a stronger sustained response compared to the 5 Hz AM tone (See Table 1). Source-derived spectral and ITPC parameters were significantly higher compared to sensor-derived parameters (Table 1, all sensor vs. source paired t-tests $p < 0.001$). Transient responses at frequencies sub-/harmonic to 5 and 40 Hz stimuli were also observed, particularly in the 10 Hz range in the spectral time–frequency representation.

Excluding the initial transient stimulus onset response, spectral ASSRs to 5 Hz AM tones generally manifested as bursts of activity. Relative to spectral signal changes, ITPC measures of ASSR to 5 Hz stimulus showed more distinct synchronous activity in the 5 Hz range (Supplementary Fig. 1). A similar pattern was observed for source-derived spectral measures and ITPC values. In contrast, individual participants' ASSRs to 40 Hz manifested stronger spectral signal change and ITPC for both sensor and source signals (Supplementary Fig. 2; Table 1).

ICCs computed for spectral power varied between stimulation frequencies as well as between sensor vs. source level, with values ranging between ~0.61 and 0.82 (Fig. $5C_{(i),\,(iii)}$). ICCs were lower for the ASSRs to 5 Hz tones (ICC = 0.609; $p = 0.010$) relative to 40 Hz AM tones (ICC = 0.823; $p = 0.001$). A similar pattern can also be seen for the source-derived ASSR spectral signal changes (Fig. $5B_{(i),\,(iii)}$) with weaker ICC for ASSRs to 5 Hz (ICC = 0.745; $p = 0.001$) compared to ASSRs to 40 Hz (ICC = 0.813; $p = 0.002$) AM tones (Table 2; Fig. $5D_{(i),\,(iii)}$).

Notably, we observed consistently higher ICC values for ITPC compared to spectral signal changes across sessions with all parameters yielding ICCs >0.8 (Fig. $5_{(ii),\,(iv)}$). ICCs computed from ITPC measures were particularly robust for the 5 Hz ASSR both at sensor ($ICC_{ITPC} = 0.951$; $p < 0.0001$; $ICC_{SPECTRAL} = 0.609$; $p = 0.01$) and source levels ($ICC_{ITPC} = 0.964$; $p < 0.0001$; $ICC_{SPECTRAL} = 0.745$; $p < 0.0001$). Slightly lower values for ITPC-derived ICCs were obtained to 40 Hz AM tones which were, however, still higher (sensor: ICC = 0.937; $p << 0.0001$; source: ICC = 0.869; $p << 0.0001$) compared to spectrally derived ICCs (sensor: ICC = 0.823; $p = 0.0001$; source: ICC = 0.813; $p = 0.0002$).

We noted very similar trends in the ICCs derived from non-Gaussian-fitted parameters of interests (See Supplementary Results; Supplementary Table 1; Supplementary Fig. 3) despite observing higher ICCs for 5 Hz and slightly lower ICCs for 40 Hz ASSR parameters, relative to those derived from Gauss-fitted signals. Similarly, ICCs computed from ITPCs were consistently higher relative to those derived from spectral signal change, with a more pronounced difference for 5 Hz ASSR derived parameters.

Additionally, ICCs derived for baseline and stimulus duration (StimDur; See Supplementary Table 2) of 5 Hz ASSR spectral signals yielded high reliability for both sensor ($ICC_{BASELINE} = 0.975$; $p < 0.0001$; $ICC_{STIMDUR} = 0.979$; $p < 0.0001$) and source ($ICC_{BASELINE} = 0.976$; $p < 0.0001$; $ICC_{STIMDUR} = 0.984$; $p < 0.0001$) assessments. In contrast, lower ICCs were derived for 40 Hz ASSR baseline and stimulus duration raw spectral parameters for both sensor ($ICC_{BASELINE} = 0.489$; $p = 0.038$; $ICC_{STIMDUR} = 0.471$; $p = 0.045$) and source ($ICC_{BASELINE} = 0.466$; $p = 0.046$; $ICC_{STIMDUR} = 0.486$ $p = 0.039$) assessments (Supplementary Table 2).

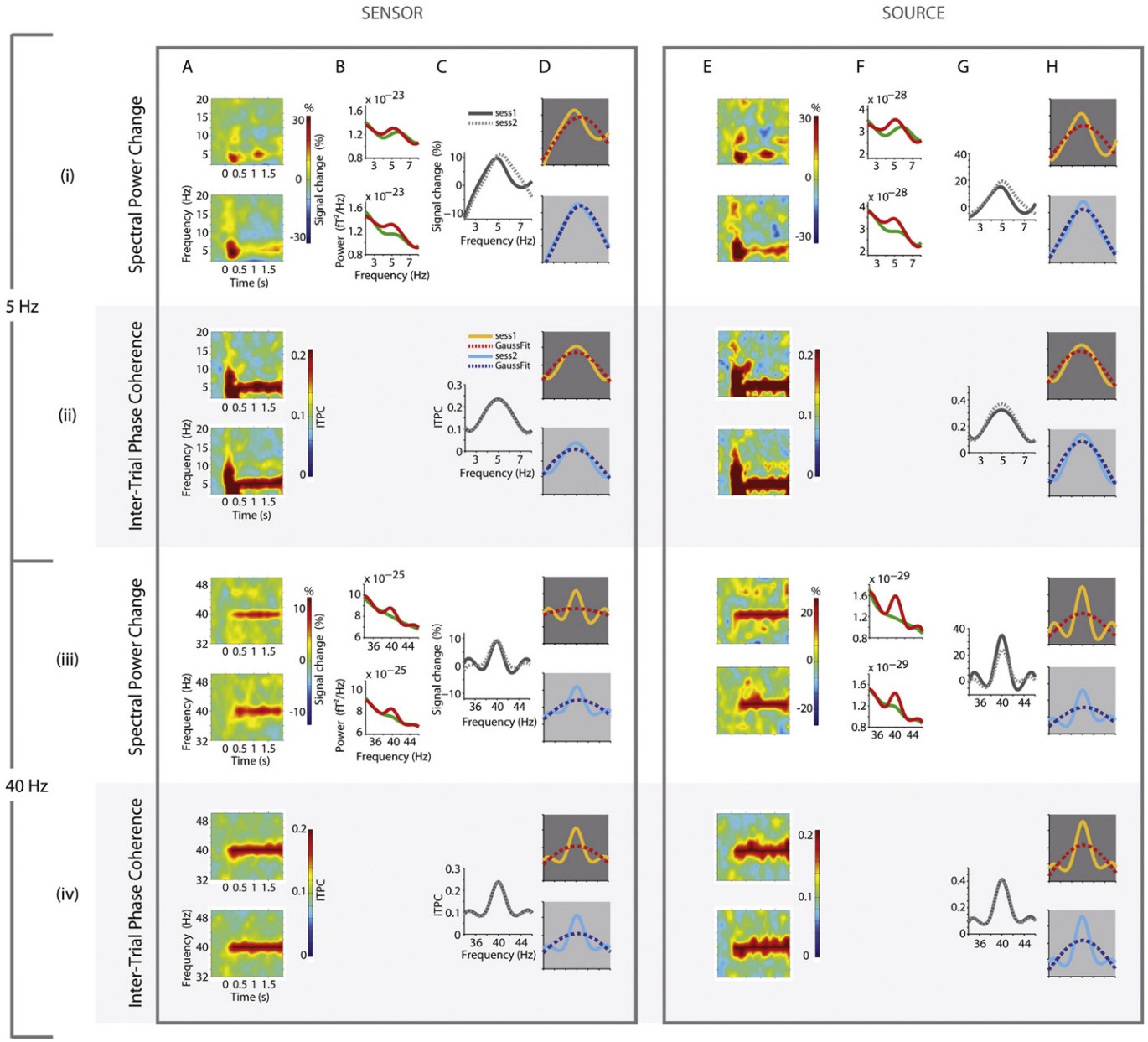

Fig. 3. Analysis approach for deriving spectral signal change and ITPC retest parameters. Overview of analysis approach illustrated with data from 1 participant (s2). For each participant, power signal change relative to baseline (i, iii) and ITPC (ii, iv) were derived for each MEG session (session 1—upper, and session 2—bottom rows, respectively), and for 5 Hz (i–ii) and 40 Hz (iii–iv) ASSR stimuli. (A) Time–frequency plots for signal change or ITPC and where appropriate, (B) the corresponding baseline (green) and stimulus-related (red) signals are depicted for both MEG sessions for 5 Hz (2–8 Hz) and 40 Hz (34–46 Hz). Relative change in spectral data for both (C) and each separate session (D) are shown (solid = ASSR parameter time series; dotted = fitted Gauss; darker and lighter grey plot background for session 1 and 2, respectively), from which the fitted ASSR parameter at stimulus frequency (i.e. 5 Hz or 40 Hz) was extracted for reliability assessment for both sensor (A–D) and source (E–H) derived neuromagnetic signals. Intensity scaling for time–frequency plots is the same as for Supplementary Figs. 1 and 2. Refer to *Methods* for further details.

Discussion

The goal of this study was to examine the test–retest reliability of frequency-specific ASSRs to 5 Hz and 40 Hz AM tones from MEG data recorded over two sessions. Our results for spectral signal change and ITPC parameters suggest highly reproducible oscillatory signatures for both sensor and estimated source signals (mean ICC = 0.839), highlighting the accuracy and robustness of MEG approaches to assess both amplitude modulation and precise phase-locking during auditory stimulation. Furthermore, our findings indicate that ITPC values may be more reliable compared to relative power change in quantifying ASSR across sessions. The current data support and extend previous findings on test–retest reliability of oscillatory signatures using MEG (e.g. Deuker et al., 2009; Muthukumaraswamy et al., 2010) and EEG (e.g. Fründ et al., 2007; Keil et al., 2003; McEvoy et al., 2000; McFadden et al., 2014).

Compared to previous EEG/MEG studies, we presented AM tones of longer duration (2000 ms vs. 500 ms) because ASSR is known to be elicited at least 240 ms post-stimulus onset (Ross et al., 2002). As a result, the time-window for our analysis is well outside the transient evoked response and therefore the overall level of response amplitude reflects the capacity of the neural system to resonate at the AM stimulus frequencies. Consistent with prior findings, we found that the modulation of amplitude and phase-locking was higher to stimulation at 40 Hz compared to 5 Hz (Hamm et al., 2011, 2012; Krishnan et al., 2009). These data suggest that 40 Hz may constitute the preferred

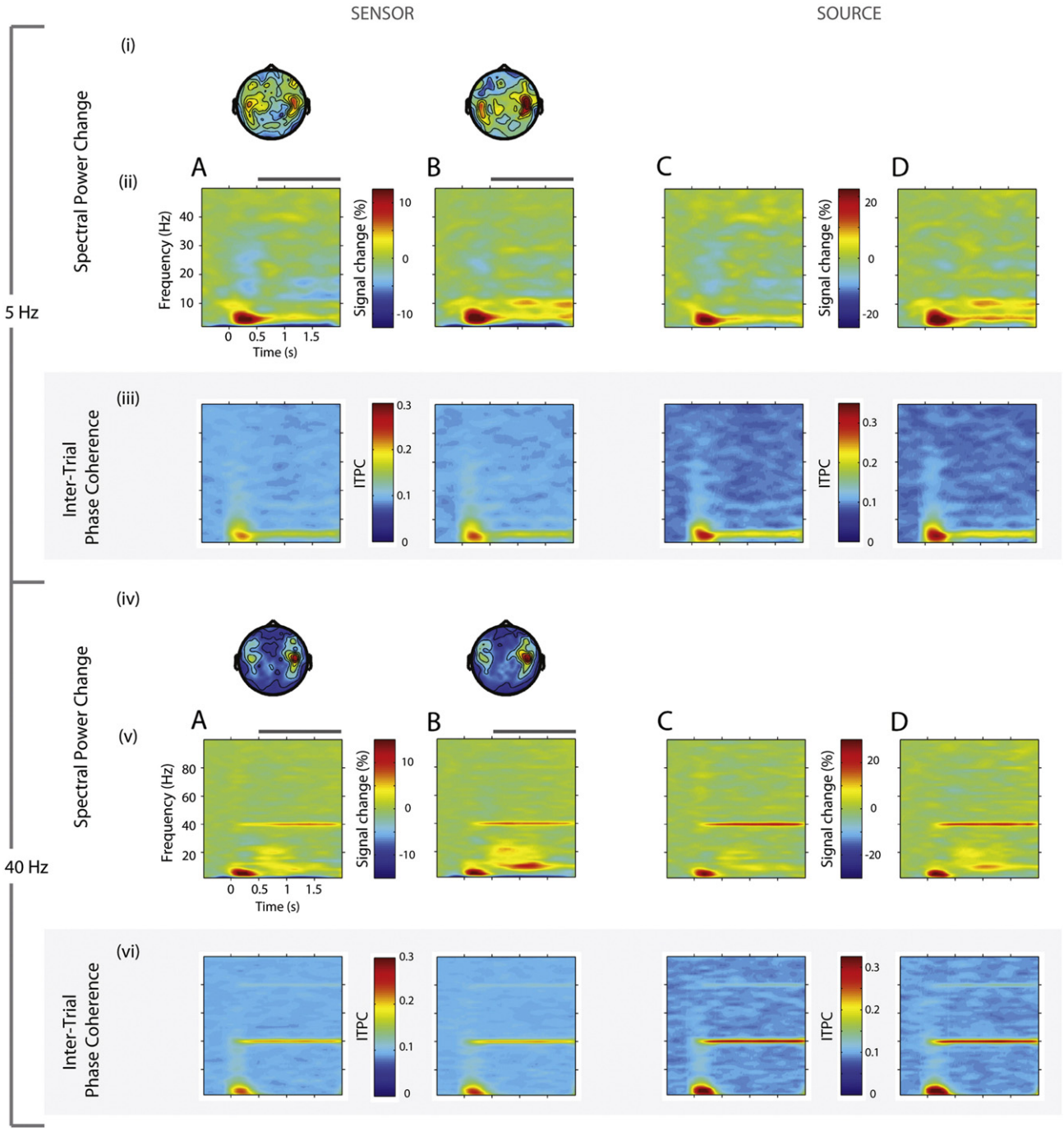

Fig. 4. Grand average auditory steady-state responses for each MEG session. Topographies of 5 Hz (i) and 40 Hz (iv) relative power change for MEG session 1 (A) and 2 (B) are averaged across all participants and over the duration of interest 0.5–2 s, as indicated by the horizontal grey bars (ii, v). Power signal change relative to baseline for 5 Hz (ii) and 40 Hz (v), as well as ITPC at 5 Hz (iii) and at 40 Hz (vi) are averaged across participants separately for signals derived at sensor (A,B) and at source (C, D) space for both MEG sessions (1 and 2, respectively).

resonance frequency of oscillatory networks in auditory cortices (Azzena et al., 1995; Brenner et al., 2009; Galambos et al., 1981; Picton et al., 2003).

Interestingly, we observed that the reproducibility of absolute power values for baseline and stimulation periods varied with ASSR stimulus as well as their corresponding baseline-corrected spectral measures. Although absolute spectral power at 5 Hz baseline and stimulus duration exhibited robust repeatability, baseline-corrected spectral power yielded lower reliability. The opposite was observed for 40 Hz ASSR, in which absolute spectral signal for baseline and stimulus duration yielded average reliability compared to its highly reliable baseline-corrected spectral signal. One reason for this difference may be due to the power law ($^1/_f$) scaling manifested in brain signals (Bédard et al., 2006). Relative to higher frequencies (e.g. 40 Hz), lower frequency (e.g. 5 Hz) signals exhibit stronger spectral power. As such, a variable measure of 5 Hz ASSR stimulus-induced effects can arise from a modest signal change relative to an existing strong baseline power. In the case of 40 Hz ASSR stimulation, a weak baseline power followed by a comparatively strong increase after stimulus onset can yield a more robust relative change measure. Our observations of relative spectral signal changes support the notion that ASSRs are generated in addition to ongoing spontaneous activity and are facilitated when underlying neural networks are entrained to rhythmic stimulation close to their best-tuned frequency (Ross et al., 2005).

Table 1
Summary of participants' 5 Hz and 40 Hz ASSR spectral signal modulation (%) and instantaneous inter-trial phase-coherence (ITPC) measures for each MEG session at sensor and source levels. Within participant statistical comparisons of sensor vs. source measures highlight significant differences ($p < 0.05$). Refer to *Results* for further details.

	ASSR		Sensor level		Source level			Sensor vs. Source	
		Session	1	2	1	2		1	2
Spectral Signal Change (%)	**5 Hz**	**mean**	4.460	5.380	7.900	10.860	t_{12}	−3.639	−2.991
		± sd	2.740	6.170	5.740	12.290	***p***	0.003	0.011
	40 Hz	**mean**	6.090	6.770	14.910	13.840	t_{12}	−3.557	−4.123
		± sd	5.330	5.950	13.780	11.280	***p***	0.004	0.001
Inter-Trial Phase Coherence (ITPC)	**5 Hz**	**mean**	0.158	0.160	0.205	0.211	t_{12}	−4.488	−4.610
		± sd	0.027	0.031	0.062	0.069	***p***	0.001	0.001
	40 Hz	**mean**	0.189	0.188	0.252	0.250	t_{12}	−4.969	−5.074
		± sd	0.052	0.047	0.084	0.077	***p***	3.26E−04	2.73E−04

ICC values for ITPC measures during ASSRs were consistently higher compared to spectral changes for both sensor- and source-derived measures. This was particularly evident for ASSRs to 5 Hz stimulation, which was characterized by irregular bursts of activity and could have potentially contributed to more spectral variability across sessions. As ITPC indexes the consistency with which the trial-to-trial phase of

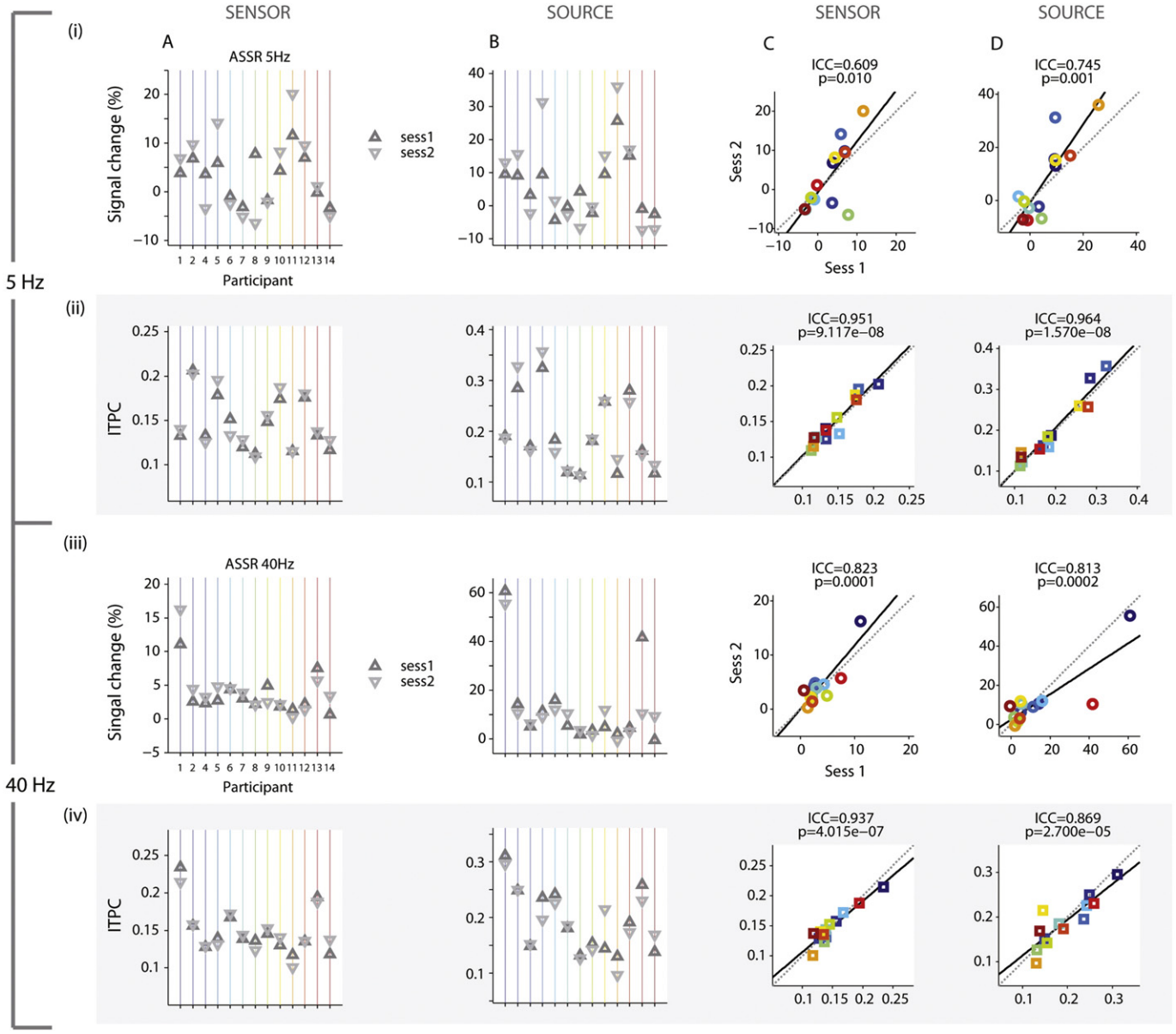

Fig. 5. Summary of test–retest reliability and corresponding intraclass correlations (ICCs). Individual parameter values for 5 Hz (i–ii) or 40 Hz (iii–iv) ASSR stimuli are extracted for each MEG session at sensor (A) and source (B) space. Test–retest reliability was assessed with ICCs and the corresponding results are summarized in (C) and (D) for sensor- and source-derived ASSR parameters.

Table 2
Summary of reliability assessments. The spectral signal modulation (%) and inter-trial phase coherence (ITPC) measures show comparably high intraclass correlations (ICC) at sensor and source levels for both 5 Hz and 40 Hz ASSR. Notably, ITPC measures yielded higher reliability compared to spectral signal change.

	ASSR		Sensor				Source		
			ICC	LB	UB		ICC	LB	UB
Spectral Signal Change (%)	**5 Hz**	***r***	0.609	0.113	0.862	***r***	0.745	0.352	0.915
		p	0.010			***p***	0.001		
	40 Hz	***r***	0.823	0.518	0.943	***r***	0.813	0.495	0.939
		p	1.49E-04			***p***	2.04E-04		
Inter-Trial Phase Coherence (ITPC)	**5 Hz**	***r***	0.951	0.848	0.985	***r***	0.964	0.885	0.989
		p	9.12E-08			***p***	1.57E-08		
	40 Hz	***r***	0.937	0.807	0.980	***r***	0.869	0.627	0.958
		p	4.01E-07			***p***	2.70E-05		

neural oscillations is temporally coupled to sensory stimulation, our data suggest that measures of phase-locked rhythmic activity may also reflect a robust spectral fingerprint, particularly for lower oscillatory frequencies.

Higher ICC values for ITPC measures of ASSRs are consistent with the EEG findings by McFadden et al. (2014) who assessed evoked spectral change and ITPC over a broad frequency range (30–120 Hz; 2.5 Hz resolution) and stimulus duration (500 ms; 20 ms resolution) using Pearson's product–moment correlation. In our study, we examined the within-subject consistency in spectral signal changes and ITPC measures of ASSR at the corresponding stimulus AM frequency for MEG sensor- and source-derived signals using the intraclass correlation (ICC). ICCs have been employed in fMRI reliability assessments (e.g. Plichta et al., 2012; Zuo et al., 2010a; 2010b) and by other MEG studies assessing the heritability (van Pelt et al., 2012) and repeatability (Muthukumaraswamy et al., 2010) of visually elicited peak gamma band response. Although the use of ICC to assess test–retest reliability is not without its limitations (e.g. see Bennett et al., 2009; Patton et al., 2005 for review), it has advantages over Pearson's product–moment correlation, which is useful for determining the relationship between two variables but less appropriate in assessing the consistency of a variable of interest.

Sensor-level-derived ICC values, particularly for ITPC, were of similar magnitude or only marginally lower than source-derived ICCs. Monitoring participants' head and MEG sensors' positioning is challenging and can contribute to differences between and within measurements in spectral power and ITPC values estimates as participants are unlikely to be in the exact same position across repeated runs. Such head positioning issue is less of a concern for the established 10–20 system adopted in EEG or MEG systems and experimental setup that allow for continuous head position information monitoring (cHPI) for subsequent analytical adjustment (e.g. Deuker et al., 2009). Given the importance of head positioning for repeated assessments at sensor level, MEG source reconstruction offers the prospect of reliability assessment of neural parameters without the precision of head re-positioning. Although previous MEG research suggested that source reconstruction may improve the reliability of auditory evoked P50 responses (Lu et al., 2007), our data suggest that careful monitoring of participants' head and sensors' positioning can yield robust sensor-derived estimates of ITPC and spectral modulation in MEG data.

While sensor-derived measures of ASSR might expedite signal processing, particularly for large population studies, the inherent volume conductance implies that signals acquired from any one sensor can arise from a combination of sources that are not restricted to a single hemisphere. To this end, source-estimated signals would also be helpful for assessing laterality effects in ASSRs, e.g. as have been reported in ScZ (Edgar et al., 2014; Hamm et al., 2011; Hirano et al., 2015; Spencer et al., 2009; Teale et al., 2008). Since addressing differences in lateralization was outside the scope of the present study, we focused our assessment of ASSRs bilaterally such that there was a correspondence between results obtained for sensor level and source space. Nonetheless, our data support the advantages of using source reconstruction for the assessment of ASSRs as evidenced by the higher signal-to-noise (SNR) obtained for source vs. sensor estimates, particularly observed in the ~80–140% increase for spectral power changes. Additionally, the observed improvements in spectral test–retest reliability from source-derived signals may be attributed to the beamforming approach, which acts as spatial filters in suppressing background activity that may lower the reliability of sensor signals, particularly in the case of 5 Hz ASSR.

Conclusion

The present study provides further evidence for the reliability of MEG-derived oscillatory signatures during auditory processing. Specifically, our findings highlight that ITPC is a particularly robust parameter of rhythmic activity and could potentially be used as a spectral fingerprint. ASSRs are well suited for translational research as ASSR parameters can be obtained from animal models of psychiatric conditions with the potential to inform our understanding of the underlying pathophysiological processes of disorders such as ScZ and ASDs (e.g. Sivarao, 2015). Our research demonstrates that MEG-based read-outs of neural oscillations are suitable for longitudinal studies and underscore the utility of MEG in basic and clinical research.

Acknowledgments

We are grateful to the two anonymous reviewers for their helpful suggestions in improving our manuscript; A Bahmer and B Giordano for valuable insights during the development and assessment of acoustic parameters; R Ince for sharing his computational expertise in efficiently determining the dominant orientation of each source's signals derived with eLORETA; I Delis for helpful suggestions in using Gaussian fitting parameters; G Rousselet for references on ICC and statistics; H Hult Skogs for assisting with participant recruitment and experimental piloting; G Paterson for MEG facility troubleshooting; F Crabbe for her invaluable help in acquiring participants' anatomical MRIs. This study was funded by the University of Glasgow. PJU receives research funding from Lilly UK.

Appendix A. Supplementary data

Supplementary data to this article can be found online at http://dx.doi.org/10.1016/j.neuroimage.2015.07.055.

References

Akam, T., Kullmann, D.M., 2014. Oscillatory multiplexing of population codes for selective communication in the mammalian brain. Nat. Rev. Neurosci. 15 (2), 111–122.
Azzena, G.B., Conti, G., Santarelli, R., Ottaviani, F., Paludetti, G., Maurizi, M., 1995. Generation of human auditory steadystate responses (SSRs). I: Stimulus rate effects. Hear. Res. 83 (1–2), 1–8.
Bartos, M., Vida, I., Jonas, P., 2007. Synaptic mechanisms of synchronized gamma oscillations in inhibitory interneuron networks. Nat. Rev. Neurosci. 8 (1), 45–56.
Bastiaansen, M.C., Knosche, T.R., 2000. Tangential derivative mapping of axial MEG applied to event-related desynchronization research. Clin. Neurophysiol. 111 (7), 1300–1305.
Bédard, C., Kröger, H., Destexhe, A., 2006. Does the 1/f frequency scaling of brain signals reflect self-organized critical states? Phys. Rev. Lett. 97 (11), 118102.
Bennett, C.M., Wolford, G.L., Miller, M.B., 2009. The principled control of false positives in neuroimaging. Soc. Cogn. Affect. Neurosci. 4 (4), 417–422.
Boutros, N.N., Overall, J., Zouridakis, G., 1991. Test–retest reliability of the P50 mid-latency auditory evoked response. Psychiatry Res. 39 (2), 181–192.
Brenner, C.A., Sporns, O., Lysaker, P.H., O'Donnell, B.F., 2003. EEG synchronization to modulated auditory tones in schizophrenia, schizoaffective disorder, and schizotypal personality disorder. Am. J. Psychiatry 160 (12), 2238–2240.
Brenner, C.A., Krishnan, G.P., Vohs, J.L., Ahn, W., Hetrick, W.P., Morzorati, S.L., O'Donnell, B.F., 2009. Steady state responses: Electrophysiological assessment of sensory function in schizophrenia. Schizophr. Bull. 35, 1065–1077.

Brunel, N., Wang, X., 2003. What determines the frequency of fast network oscillations with irregular neural discharges?I. synaptic dynamics and excitation-inhibition balance. J. Neurophysiol. 90 (1), 415–430.
Buzsáki, G., Wang, X., 2012. Mechanisms of gamma oscillations. Annu. Rev. Neurosci. 35 (1), 203–225.
Buzsáki, G., Watson, B.O., 2012. Brain rhythms and neural syntax: Implications for efficient coding of cognitive content and neuropsychiatric disease. Dialogues Clin. Neurosci. 14 (4), 345–367.
Campbell, A.E., Sumner, P., Singh, K.D., Muthukumaraswamy, S.D., 2014. Acute effects of alcohol on stimulus-induced gamma oscillations in human primary visual and motor cortices. Neuropsychopharmacology 39 (9), 2104–2113.
Canolty, R.T., Knight, R.T., 2010. The functional role of cross-frequency coupling. Trends Cogn. Sci. 14 (11), 506–515.
Cardenas, V.A., Gerson, J., Fein, G., 1993. The reliability of P50 suppression as measured by the conditioning/testing ratio is vastly improved by dipole modeling. Biol. Psychiatry 33 (5), 335–344.
Cardin, J.A., Carlen, M., Meletis, K., Knoblich, U., Zhang, F., Deisseroth, K., Tsai, L., Moore, C.I., 2009. Driving fast-spiking cells induces gamma rhythm and controls sensory responses. Nature 459 (7247), 663–667.
David, O., Kilner, J.M., Friston, K.J., 2006. Mechanisms of evoked and induced responses in MEG/EEG. NeuroImage 31 (4), 1580–1591.
Deuker, L., Bullmore, E.T., Smith, M., Christensen, S., Nathan, P.J., Rockstroh, B., Bassett, D.S., 2009. Reproducibility of graph metrics of human brain functional networks. NeuroImage 47 (4), 1460–1468.
Edgar, J.C., Chen, Y., Lanza, M., Howell, B., Chow, V.Y., Heiken, K., Liu, S., Wootton, C., Hunter, M.A., Huang, M., et al., 2014. Cortical thickness as a contributor to abnormal oscillations in schizophrenia? NeuroImage: Clin. 4 (0), 122–129.
Fries, P., 2005. A mechanism for cognitive dynamics: Neuronal communication through neuronal coherence. Trends Cogn. Sci. 9 (10), 474–480.
Fründ, I., Schadow, J., Busch, N.A., Körner, U., Herrmann, C.S., 2007. Evoked γ oscillations in human scalp EEG are test–retest reliable. Clin. Neurophysiol. 118 (1), 221–227.
Galambos, R., Makeig, S., Talmachoff, P.J., 1981. A 40-hz auditory potential recorded from the human scalp. Proc. Natl. Acad. Sci. 78 (4), 2643–2647.
Georgopoulos, A.P., Tan, H.-R.M., Lewis, S.M., Leuthold, A.C., Winskowski, A.M., Lynch, J.K., Engdahl, B., 2010. The synchronous neural interactions test as a functional neuromarker for post-traumatic stress disorder (PTSD): A robust classification method based on the bootstrap. J. Neural Eng. 7, 016011.
Gonzalez-Burgos, G., Lewis, D.A., 2008. GABA neurons and the mechanisms of network oscillations: Implications for understanding cortical dysfunction in schizophrenia. Schizophr. Bull. 34 (5), 944–961.
Gray, C.M., Singer, W., 1989. Stimulus-specific neuronal oscillations in orientation columns of cat visual cortex. Proc. Natl. Acad. Sci. U. S. A. 86 (5), 1698–1702.
Griskova-Bulanova, I., Griksiene, R., Korostenskaja, M., Ruksenas, O., 2014. 40 hz auditory steady-state response in females: When is it better to entrain? Acta Neurobiol. Exp. 74, 91–97.
Gross, J., Hoogenboom, N., Thut, G., Schyns, P., Panzeri, S., Belin, P., Garrod, S., 2013. Speech rhythms and multiplexed oscillatory sensory coding in the human brain. PLoS Biol. 11 (12), e1001752.
Haegens, S., Cousijn, H., Wallis, G., Harrison, P.J., Nobre, A.C., 2014. Inter- and intra-individual variability in alpha peak frequency. NeuroImage 92 (0), 46–55.
Hamm, J.P., Gilmore, C.S., Picchetti, N.A.M., Sponheim, S.R., Clementz, B.A., 2011. Abnormalities of neuronal oscillations and temporal integration to low- and high-frequency auditory stimulation in schizophrenia. Biol. Psychiatry 69 (10), 989–996.
Hamm, J.P., Gilmore, C.S., Clementz, B.A., 2012. Augmented gamma band auditory steady-state responses: Support for NMDA hypofunction in schizophrenia. Schizophr. Res. 138 (1), 1–7.
Hashimoto, T.M.D., Bazmi, H.H.M.S., Mirnics, K.M.D., Wu, Q.P.D., Sampson, A.R.P.D., Lewis, D.A.M.D., 2008. Conserved regional patterns of GABA-related transcript expression in the neocortex of subjects with schizophrenia. Am. J. Psychiatr. 165 (4), 479–489.
Helfrich, R.F., Knepper, H., Nolte, G., Strüber, D., Rach, S., Herrmann, C.S., Schneider, T.R., Engel, A.K., 2014. Selective modulation of interhemispheric functional connectivity by HD-tACS shapes perception. PLoS Biol. 12 (12), e1002031.
Hirano, Y., Oribe, N., Kanba, S., Onitsuka, T., Nestor, P.G., Spencer, K.M., 2015. Spontaneous gamma activity in schizophrenia. JAMA Psychiatry. http://dx.doi.org/10.1001/jamapsychiatry.2014.2642.
Hong, L.E., Summerfelt, A., McMahon, R., Adami, H., Francis, G., Elliott, A., Buchanan, R.W., Thaker, G.K., 2004. Evoked gamma band synchronization and the liability for schizophrenia. Schizophr. Res. 70 (2–3), 293–302.
Jerger, K., Biggins, C., Fein, G., 1992. P50 suppression is not affected by attentional manipulations. Biol. Psychiatry 31 (4), 365–377.
Kathmann, N., Engel, R.R., 1990. Sensory gating in normals and schizophrenics: A failure to find strong P50 suppression in normals. Biol. Psychiatry 27 (11), 1216–1226.
Keil, A., Stolarova, M., Heim, S., Gruber, T., Müller, M., 2003. Temporal stability of high-frequency brain oscillations in the human EEG. Brain Topogr. 16 (2), 101–110.
Krishnan, G.P., Hetrick, W.P., Brenner, C.A., Shekhar, A., Steffen, A.N., O'Donnell, B.F., 2009. Steady state and induced auditory gamma deficits in schizophrenia. NeuroImage 47 (4), 1711–1719.
Kwon, J.S., O'Donnell, B.F., Wallenstein, G.V., Greene, R.W., Hirayasu, Y., Nestor, P.G., Hasselmo, M.E., Potts, G.F., Shenton, M.E., McCarley, R.W., 1999. Gamma frequency–range abnormalities to auditory stimulation in schizophrenia. Arch. Gen. Psychiatry 56 (11), 1001–1005.
Lamberti, J.S., Schwarzkopf, S.B., Boutros, N., Crilly, J.F., Martin, R., 1993. Within-session changes in sensory gating assessed by p50 evoked potentials in normal subjects. Prog. Neuro-Psychopharmacol. Biol. Psychiatry 17 (5), 781–791.
Light, G.A., Hsu, J.L., Hsieh, M.H., Meyer-Gomes, K., Sprock, J., Swerdlow, N.R., Braff, D.L., 2006. Gamma band oscillations reveal neural network cortical coherence dysfunction in schizophrenia patients. Biol. Psychiatry 60 (11), 1231–1240.
Lopes da Silva, F., 2013. EEG and MEG: Relevance to neuroscience. Neuron 80, 1112–1128.
Lu, B.Y., Edgar, J.C., Jones, A.P., Smith, A.K., Huang, M., Miller, G.A., Cañive, J.M., 2007. Improved test–retest reliability of 50-ms paired-click auditory gating using magneto-encephalography source modeling. Psychophysiology 44 (1), 86–90.
McEvoy, L.K., Smith, M.E., Gevins, A., 2000. Test–retest reliability of cognitive EEG. Clin. Neurophysiol. 111 (3), 457–463.
McFadden, K.L., Steinmetz, S.E., Carroll, A.M., Simon, S.T., Wallace, A., Rojas, D.C., 2014. Test–retest reliability of the 40 hz EEG auditory steady-state response. PLoS ONE 9 (1), e85748.
McGraw, K.O., Wong, S.P., 1996a. Forming inferences about some intraclass correlation coefficients. Psychol. Methods 1 (1), 30–46.
McGraw, K.O., Wong, S.P., 1996b. Forming inferences about some intraclass correlations coefficients': Correction. Psychol. Methods 1 (4), 390.
Moyer, C.E., Delevich, K.M., Fish, K.N., Asafu-Adjei, J.K., Sampson, A.R., Dorph-Petersen, K., Lewis, D.A., Sweet, R.A., 2012. Reduced glutamate decarboxylase 65 protein within primary auditory cortex inhibitory boutons in schizophrenia. Biol. Psychiatry 72 (9), 734–743.
Muthukumaraswamy, S.D., Singh, K.D., Swettenham, J.B., Jones, D.K., 2010. Visual gamma oscillations and evoked responses: Variability, repeatability and structural MRI correlates. NeuroImage 49 (4), 3349–3357.
Oldfield, R.C., 1971. The assessment and analysis of handedness: The Edinburgh Inventory. Neuropsychologia 9 (1), 97–113.
Oostenveld, R., Fries, P., Maris, E., Schoffelen, J., 2011. FieldTrip: Open source software for advanced analysis of MEG, EEG, and invasive electrophysiological data. Comput. Intell. Neurosci. 2011. http://dx.doi.org/10.1155/2011/156869.
Pantev, C., Roberts, L.E., Elbert, T., Ross, B., Wienbruch, C., 1996. Tonotopic organization of the sources of human auditory steady-state responses. Hear. Res. 101 (1–2), 62–74.
Pascual-Marqui, R.D., 2007. Discrete, 3D distributed, linear imaging methods of electric neuronal activity. part 1: Exact, zero error localization. ArXiv (Preprint arXiv:0710.3341).
Pascual-Marqui, R.D., Lehmann, D., Koukkou, M., Kochi, K., Anderer, P., Saletu, B., Tanaka, H., Hirata, K., John, E.R., Prichep, L., et al., 2011. Assessing interactions in the brain with exact low-resolution electromagnetic tomography. Philos. Trans. A Math. Phys. Eng. Sci. 369 (1952), 3768–3784.
Patton, N., Aslam, T., Murray, G., 2005. Statistical strategies to assess reliability in ophthalmology. Eye (Lond.) 20 (7), 749–754.
Picton, T.W., John, M.S., Dimitrijevic, A., Purcell, D., 2003. Human auditory steady-state responses: Respuestas auditivas de estado estable en humanos. Int. J. Audiol. 42 (4), 177–219.
Plichta, M.M., Schwarz, A.J., Grimm, O., Morgen, K., Mier, D., Haddad, L., Gerdes, A.B.M., Sauer, C., Tost, H., Esslinger, C., et al., 2012. Test–retest reliability of evoked BOLD signals from a cognitive–emotive fMRI test battery. NeuroImage 60 (3), 1746–1758.
Rass, O., Forsyth, J.K., Krishnan, G.P., Hetrick, W.P., Klaunig, M.J., Breier, A., O'Donnell, B.F., Brenner, C.A., 2012. Auditory steady state response in the schizophrenia, first-degree relatives, and schizotypal personality disorder. Schizophr. Res. 136 (1–3), 143–149.
Regan, D., 1989. Human brain electrophysiology: Evoked potentials and evoked magnetic fields in science and medicine. Elsevier, New York.
Rojas, D., Teale, P., Maharajh, K., Kronberg, E., Youngpeter, K., Wilson, L., Wallace, A., Hepburn, S., 2011. Transient and steady-state auditory gamma-band responses in first-degree relatives of people with autism spectrum disorder. Mol. Autism 2 (1), 11.
Roopun, A.K., Kramer, M.A., Carracedo, L.M., Kaiser, M., Davies, C.H., Traub, R.D., Kopell, N.J., Whittington, M.A., 2008. Temporal interactions between cortical rhythms. Front. Neurosci. 2 (2), 145–154.
Ross, B., Borgmann, C., Draganova, R., Roberts, L.E., Pantev, C., 2000. A high-precision magnetoencephalographic study of human auditory steady-state responses to amplitude-modulated tones. J. Acoust. Soc. Am. 108 (2), 679–691.
Ross, B., Picton, T.W., Pantev, C., 2002. Temporal integration in the human auditory cortex as represented by the development of the steady-state magnetic field. Hear. Res. 165 (1–2), 68–84.
Ross, B., Herdman, A.T., Pantev, C., 2005. Stimulus induced desynchronization of human auditory 40-hz steady-state responses. J. Neurophysiol. 94 (6), 4082–4093.
Rouhinen, S., Panula, J., Palva, J.M., Palva, S., 2013. Load dependence of β and γ oscillations predicts individual capacity of visual attention. J. Neurol. Sci. 33, 19023–19033.
Roux, F., Wibral, M., Mohr, H.M., Singer, W., Uhlhaas, P.J., 2012. Gamma-band activity in human prefrontal cortex codes for the number of relevant items maintained in working memory. J. Neurosci. 32 (36), 12411–12420.
Salarian, A., 2008. http://www.mathworks.com/matlabcentral/fileexchange/22099-intraclass-correlation-coefficient–icc.
Schnitzler, A., Gross, J., 2005. Normal and pathological oscillatory communication in the brain. Nat. Rev. Neurosci. 6 (4), 285–296.
Shrout, P.E., Fleiss, J.L., 1979. Intraclass correlations: Uses in assessing rater reliability. Psychol. Bull. 86 (2), 420–428.
Siegel, M., Donner, T.H., Engel, A.K., 2012. Spectral fingerprints of large-scale neuronal interactions. Nat. Rev. Neurosci. 13 (2), 121–134.
Sivarao, D.V., 2015. The 40-hz auditory steady-state response: A selective biomarker for cortical NMDA function. Ann. N. Y. Acad. Sci. 1344 (1), 27–36.
Sohal, V.S., Zhang, F., Yizhar, O., Deisseroth, K., 2009. Parvalbumin neurons and gamma rhythms enhance cortical circuit performance. Nature 459 (7247), 698–702.
Spencer, K.M., Niznikiewicz, M.A., Shenton, M.E., McCarley, R.W., 2008. Sensory-evoked gamma oscillations in chronic schizophrenia. Biol. Psychiatry 63 (8), 744–747.
Spencer, K., Niznikiewicz, M., Nestor, P., Shenton, M., McCarley, R., 2009. Left auditory cortex gamma synchronization and auditory hallucination symptoms in schizophrenia. BMC Neurosci. 10 (1), 85.
Sun, L., Castellanos, N., Grützner, C., Koethe, D., Rivolta, D., Wibral, M., Kranaster, L., Singer, W., Leweke, M.F., Uhlhaas, P.J., 2013. Evidence for dysregulated high-frequency oscillations during sensory processing in medication-naïve, first episode schizophrenia. Schizophr. Res. 150 (2–3), 519–525.

Sweet, R.A., Bergen, S.E., Sun, Z., Marcsisin, M.J., Sampson, A.R., Lewis, D.A., 2007. Anatomical evidence of impaired feedforward auditory processing in schizophrenia. Biol. Psychiatry 61 (7), 854–864.

Sweet, R.A., Henteleff, R.A., Zhang, W., Sampson, A.R., Lewis, D.A., 2009. Reduced dendritic spine density in auditory cortex of subjects with schizophrenia. Neuropsychopharmacology 34 (2), 374–389.

Tada, M., Nagai, T., Kirihara, K., Koike, S., Suga, M., Araki, T., Kobayashi, T., Kasai, K., 2014. Differential alterations of auditory gamma oscillatory responses between pre-onset high-risk individuals and first-episode schizophrenia. Cereb. Cortex. http://dx.doi.org/10.1093/cercor/bhu278.

Tallon-Baudry, C., Bertrand, O., 1999. Oscillatory gamma activity in humans and its role in object representation. Trends Cogn. Sci. 3 (4), 151–162.

Tallon-Baudry, C., Bertrand, O., Delpuech, C., Pernier, J., 1996. Stimulus specificity of phase-locked and non-phase-locked 40 hz visual responses in human. J. Neurosci. 16 (13), 4240–4249.

Tan, H.-R.M., Leuthold, H., Gross, J., 2013. Gearing up for action: Attentive tracking dynamically tunes sensory and motor oscillations in the alpha and beta band. NeuroImage 82 (0), 634–644.

Teale, P., Collins, D., Maharajh, K., Rojas, D.C., Kronberg, E., Reite, M., 2008. Cortical source estimates of gamma band amplitude and phase are different in schizophrenia. NeuroImage 42 (4), 1481–1489.

Traub, R.D., Whittington, M.A., Stanford, I.M., Jefferys, J.G.R., 1996. A mechanism for generation of long-range synchronous fast oscillations in the cortex. Nature 383 (6601), 621–624.

Uhlhaas, P., Singer, W., 2012. Neuronal dynamics and neuropsychiatric disorders: Toward a translational paradigm for dysfunctional large-scale networks. Neuron 75 (6), 963–980.

van Pelt, S., Boomsma, D.I., Fries, P., 2012. Magnetoencephalography in twins reveals a strong genetic determination of the peak frequency of visually induced gamma-band synchronization. J. Neurosci. 32 (10), 3388–3392.

Wang, X., 2010. Neurophysiological and computational principles of cortical rhythms in cognition. Physiol. Rev. 90 (3), 1195–1268.

Wilson, T.W., Rojas, D.C., Reite, M.L., Teale, P.D., Rogers, S.J., 2007. Children and adolescents with autism exhibit reduced MEG steady-state gamma responses. Biol. Psychiatry 62 (3), 192–197.

Womelsdorf, T., Schoffelen, J., Oostenveld, R., Singer, W., Desimone, R., Engel, A.K., Fries, P., 2007. Modulation of neuronal interactions through neuronal synchronization. Science 316 (5831), 1609–1612.

Zuo, X., Kelly, C., Adelstein, J.S., Klein, D.F., Castellanos, F.X., Milham, M.P., 2010a. Reliable intrinsic connectivity networks: Test–retest evaluation using ICA and dual regression approach. NeuroImage 49 (3), 2163–2177.

Zuo, X., Di Martino, A., Kelly, C., Shehzad, Z.E., Gee, D.G., Klein, D.F., Castellanos, F.X., Biswal, B.B., Milham, M.P., 2010b. The oscillating brain: Complex and reliable. NeuroImage 49 (2), 1432–1445.